

SYNTHESIS OF NEW RU(II) COMPLEXES AS CATALYSTS FOR NITRILE HYDRATION AND ALKENE EPOXIDATION

Universitat de Girona

Àrea de Química Inorgànica

Alba Arenas Miquel

Marisa Romero
Montse Rodríguez

Memòria del Treball de Fi de Grau
Setembre 2016

Index

Resum	i
Resumen	ii
Summary	iii
Abbreviations	iv
1. Introduction	1
1.1 Generalities of ruthenium	1
1.2 Ruthenium polypyridine aqua complexes	1
1.3 Ruthenium complexes with sulfoxide ligands	2
1.3.1 Ru-dmso bond	3
1.4 Ruthenium-chloro complexes as catalysts	4
1.4.1 Hydrolysis of nitriles	4
1.4.2 Alkene epoxidation	5
2. Objectives	7
3. Experimental section	8
3.1 Instrumentation and measurements	8
3.2 Synthesis of the compounds	8
3.2.1 Synthesis of chloro-complex	10
3.2.2 Synthesis of aqua-complex	11
3.2.3 Catalytic experiments	11
3.2.3.1 Hydrolysis of nitriles	11
3.2.3.2 Alkene epoxidation	12
4. Results and discussion	13
4.1 Synthesis and structures	13
4.2 Spectroscopic properties	14
4.2.1 IR spectroscopy	14
4.2.2 NMR spectroscopy	15
4.2.3 UV-Vis spectroscopy	18
4.2.4 Acid-base spectrophotometric titration of complex [6]	18
4.3 Electrochemical properties	20
4.4 Catalytic activity	23
4.4.1 Hydrolysis of nitriles	23
4.4.2 Alkene epoxidation	24
4.5 Ethical and sustainability	24
5. Conclusions	26
6. References	27

Resum

Durant l'experiència en el grup de recerca en la síntesis de complexos de ruteni amb lligands tipus N-donors i la seva aplicació en catàlisi, en aquest treball s'han desenvolupat diferents rutes per obtenir nous complexos de ruteni utilitzant diferents lligands N-donors i posteriorment s'ha avaluat la seva eficiència com a catalitzadors per la hidròlisi de nitrils i l'epoxidació d'alquens.

Inicialment, s'ha sintetitzat un dels lligands N-donors no comercial (pypzH) i, utilitzant en tots els casos el lligand terpiridina, per tal de formar els productes de partida ($[\text{RuCl}_2(\text{dmsO})_2(\text{pypzH})]$, $[\text{RuCl}_3(\text{trpy})]$ i $[\text{RuCl}_2(\text{dmsO})(\text{trpy})]$), s'han pogut desenvolupar tres rutes diferents per a la formació del complex de ruteni d'interès, $[\text{RuCl}(\text{trpy})(\text{pypzH})](\text{PF}_6)$. El complex s'ha caracteritzat utilitzant diferents tècniques tant espectroscòpiques com electroquímiques. Posteriorment, a partir d'aquest clorocomplex s'ha sintetitzat i caracteritzat el corresponent aquacomplex $[\text{Ru}(\text{trpy})(\text{pypzH})(\text{OH}_2)](\text{PF}_6)_2$.

Pel que fa la caracterització estructural, s'ha demostrat la formació d'un sol isòmer pel complex $[\text{RuCl}_2(\text{dmsO})_2(\text{pypzH})]$ mentre que per a $[\text{RuCl}_2(\text{dmsO})(\text{trpy})]$ s'ha obtingut una barreja de dos isòmers que es pot observar clarament en el seu espectre de RMN. Cal destacar que pel complex $[\text{RuCl}(\text{trpy})(\text{pypzH})](\text{PF}_6)$ s'obtenen també dos isòmers, *cis* i *trans*, però s'ha pogut purificar només l'isòmer *trans* per cromatografia en columna.

S'han realitzat espectres UV-Vis en diclorometà pel complex $[\text{RuCl}(\text{trpy})(\text{pypzH})](\text{PF}_6)$ on s'ha observat tant la presència de bandes MLCT com de bandes $\pi-\pi^*$ dels lligands. A més a més, s'ha realitzat una valoració espectrofotomètrica per afirmar la formació de l'aquacomplex corresponent, $[\text{Ru}(\text{trpy})(\text{pypzH})(\text{OH}_2)](\text{PF}_6)_2$, on es poden veure els desplaçaments de les bandes a mesura que varia el pH del medi aquós en que es registren els espectres.

El complex $[\text{RuCl}(\text{trpy})(\text{pypzH})](\text{PF}_6)$ ha estat caracteritzat també per tècniques electroquímiques, on s'ha pogut observar una ona reversible corresponent al parell redox Ru(III/II) del complex. Per a l'aquacomplex $[\text{Ru}(\text{trpy})(\text{pypzH})(\text{OH}_2)](\text{PF}_6)_2$, la voltametria cíclica mostra dues ones corresponents als parells Ru(IV/III) i Ru(III/II) que varien el seu valor de potencial en funció del pH.

Per acabar, s'ha avaluat l'activitat catalítica del complex $[\text{RuCl}(\text{trpy})(\text{pypzH})](\text{PF}_6)$ en la hidròlisi de nitrils i l'epoxidació d'alquens, cadascuna d'elles utilitzant dos substrats diferents. Els resultats obtinguts per ambdues catàlisis són bons o moderadament bons pel que fa a conversions, i excel·lents pel que fa a la selectivitat.

Resumen

Durante la experiencia en el grupo de investigación en la síntesis de complejos de rutenio con ligandos tipo N-Donors y su aplicación en catálisis, en este trabajo se han desarrollado diferentes rutas para obtener nuevos complejos de rutenio utilizando diferentes ligandos N-Donors y posteriormente se ha evaluado su eficiencia como catalizadores para la hidrólisis de nitrilos y la epoxidación de alquenos.

Inicialmente, se ha sintetizado uno de los ligandos N-Donors no comercial (pypzH) y, utilizando en todos los casos el ligando terpiridina, para formar los productos de partida ($[\text{RuCl}_2(\text{dmsO})_2(\text{pypzH})]$, $[\text{RuCl}_3(\text{trpy})]$ y $[\text{RuCl}_2(\text{dmsO})(\text{trpy})]$), se han podido desarrollar tres rutas diferentes para la formación del complejo de rutenio de interés ($[\text{RuCl}(\text{trpy})(\text{pypzH})](\text{PF}_6)$). El complejo se ha caracterizado utilizando diferentes técnicas tanto espectroscópicas como electroquímicas. Posteriormente, a partir de este clorocomplejo se ha sintetizado y caracterizado el correspondiente aquacomplejo $[\text{Ru}(\text{trpy})(\text{pypzH})(\text{OH}_2)](\text{PF}_6)_2$.

En cuanto la caracterización estructural, se ha demostrado la formación de un solo isómero por el complejo $[\text{RuCl}_2(\text{dmsO})_2(\text{pypzH})]$ mientras que por el complejo $[\text{RuCl}_2(\text{dmsO})(\text{trpy})]$ se ha obtenido una mezcla de isómeros que se puede observar claramente en su espectro de RMN. Cabe destacar que por el complejo $[\text{RuCl}(\text{trpy})(\text{pypzH})](\text{PF}_6)$ se obtienen también dos isómeros, *cis* y *trans*, pero se ha podido purificar sólo el isómero *trans* por cromatografía en columna.

Se han realizado espectros UV-Vis en diclorometano por el complejo $[\text{RuCl}(\text{trpy})(\text{pypzH})](\text{PF}_6)$ donde se ha observado tanto la presencia de bandas MLCT como de bandas $\pi-\pi^*$ de los ligandos. Además, se ha realizado una valoración espectrofotométrica para afirmar la formación del aquacomplejo correspondiente $[\text{Ru}(\text{trpy})(\text{pypzH})(\text{OH}_2)](\text{PF}_6)_2$, donde se pueden ver los desplazamientos de las bandas a medida que varía el pH del medio acuoso en que se registran los espectros.

El complejo $[\text{RuCl}(\text{trpy})(\text{pypzH})](\text{PF}_6)$ se ha caracterizado también por técnicas electroquímicas donde se ha podido observar una onda reversible correspondiente a la pareja redox Ru(III/II) del complejo. Para el aquacomplejo $[\text{Ru}(\text{trpy})(\text{pypzH})(\text{OH}_2)](\text{PF}_6)_2$, la voltametría cíclica muestra dos ondas correspondientes a los pares Ru(IV/III) y Ru(III/II) que varían su valor de potencial en función del pH.

Por último, se ha evaluado la actividad catalítica del complejo $[\text{RuCl}(\text{trpy})(\text{pypzH})](\text{PF}_6)$ en la hidrólisis de nitrilos y la epoxidación de alquenos, cada una de ellas utilizando dos sustratos diferentes. Los resultados obtenidos por ambas catálisis, son buenos o moderadamente buenos en cuanto a conversiones, y excelentes en cuanto a la selectividad.

Summary

During this experience in the research group in the synthesis of ruthenium complexes with N-Donor ligands and their application in catalysis, in this work we have developed different pathways to obtain new ruthenium complexes using N-Donor ligands that have been and subsequently evaluated as catalysts for the hydrolysis of nitriles and alkene epoxidation.

Initially, a N-donor ligand non-commercial (pypzH) has been synthesized and, using in all cases ligand terpyridine, it has been possible to obtain the starting material ($[\text{RuCl}_2(\text{dmsO})_2(\text{pypzH})]$, $[\text{RuCl}_3(\text{trpy})]$ and $[\text{RuCl}_2(\text{dmsO})(\text{trpy})]$), and it has been developed three different pathways for the formation of the ruthenium complex of interest ($[\text{RuCl}(\text{trpy})(\text{pypzH})(\text{PF}_6)]$). The complex has been characterized using different spectroscopic and electrochemical techniques. Afterwards, from this chlorocomplexes it has been synthesized and characterized the corresponding aquacomplex $[\text{Ru}(\text{trpy})(\text{pypzH})(\text{OH}_2)](\text{PF}_6)_2$.

About structural characterization, the formation of a single isomer for $[\text{RuCl}_2(\text{dmsO})_2(\text{pypzH})]$ was obtained, while the $[\text{RuCl}_2(\text{dmsO})(\text{trpy})]$ complex was obtained a mixture of isomers which is clearly seen in NMR spectrum. Note that for $[\text{RuCl}(\text{trpy})(\text{pypzH})(\text{PF}_6)]$ complex was also obtained two isomers, *cis* and *trans*, but it had been purified only the *trans* isomer by column chromatography.

UV-Vis spectra have been performed in dichloromethane for the complex $[\text{RuCl}(\text{trpy})(\text{pypzH})(\text{PF}_6)]$, where the presence of MLCT and intraligand $\pi-\pi^*$ bands is a clear evidenced in the complex. In addition, it has performed a spectrophotometric assay to confirm the aquacomplex $[\text{Ru}(\text{trpy})(\text{pypzH})(\text{OH}_2)](\text{PF}_6)_2$ formation, where you can see the movement of the bands in front of pH variations of the aqueous medium in which the spectra are recorded.

The complex $[\text{RuCl}(\text{trpy})(\text{pypzH})(\text{PF}_6)]$ was also characterized by electrochemical techniques where a reversible wave corresponding to the Ru(III/II) redox pair have been observed. For aquacomplex $[\text{Ru}(\text{trpy})(\text{pypzH})(\text{OH}_2)](\text{PF}_6)_2$, the cyclic voltammetry was shown two waves corresponding to Ru(IV/III) and Ru(III/II) pares which was varying the potential value versus pH.

Finally, the catalytic activity the hydrolysis of nitriles and epoxidation of alkenes, of the complex $[\text{RuCl}(\text{trpy})(\text{pypzH})(\text{PF}_6)]$ has been evaluated using two different substrates. The results obtained of both catalysis, are reasonably good or good in terms of conversions and excellent in the case of selectivity.

Abbreviations

CD ₂ Cl ₂	Deuterated dichloromethane
CH ₂ Cl ₂	Dichloromethane
COSY	Correlation spectroscopy
CV	Cyclic voltammetry
d	Doublet
D ₂ O	Deuterated water
dd	Double doublet
ddd	Double double doublet
dmsO	Dimethyl sulfoxide
DPV	Differential pulse voltammetry
$E_{1/2}$	Half wave potential
GC	Gas chromatography
IR	Infrared
MHz	Megahertz
mL	Milliliters
MLCT	Metal to ligand charge transfer
mmol	Millimol
NMR	Nuclear magnetic resonance
NOESY	Nuclear overhauser effect spectroscopy
PCET	Proton-coupled-electron-transfer
pypzH	2-(3-pyrazolyl)pyridine
s	Singlet
t	Triplet
trpy	2,2',(6,6'),2"-terpyridine
UV-Vis	Ultraviolet-visible spectroscopy
V	Volts

1. Introduction

1.1 Generalities of ruthenium

Ruthenium is a metal situated in the d block of the periodic table with symbol Ru whose electronic configuration is $[\text{Kr}] 4d^7 5s^1$. A special feature of ruthenium, together with osmium, is the diversity of the oxidation states from -2, as in $[\text{Ru}(\text{CO})_2]^{2-}$, to +8 as in RuO_4 . Moreover, it can present different coordination geometries (trigonal bipyramid, octahedral...).

The kinetic stability of ruthenium complexes in different oxidation states, the often reversible nature of the redox pairs and the synthetic relative simplicity make these complexes particularly interesting. In addition, the ruthenium coordination compounds are characterized for their high electron transfer capacity,¹ their relatively low redox potential values and their ability to stabilize reactive species like oxo-metals² and metal-carbene complexes.³

Apart from the redox properties is also very significant the coordination sphere of the metal when designing an application for the compound. Ruthenium complexes with π -conjugate ligands or systems that present a type of ligands which allow the electronic delocalization have shown specific properties in nonlinear optics,⁴ molecular sensors,⁵ magnetism⁶ and liquid crystals.⁷ Furthermore, ruthenium complexes with heterocyclic N-donor ligands are the most used due to their interesting spectroscopic, photophysical and electrochemical properties.⁸ Therefore, as a result, a wide area of applications has been developed, such as molecular electronic devices,⁹ photosensitizers for the photoactive conversion of solar energy¹⁰ and photoactive DNA cleavage agents for therapeutic purposes.¹¹

1.2 Ruthenium polypyridine aqua complexes

Polypyridine complexes are coordination complexes containing polypyridine ligands. Extensive coordination chemistry about hexacoordinated complexes has been used due their high stability against oxidation and their great coordinative capacity, increased by their chelate effect (enhanced affinity of chelating ligands for a metal ion). This kind of ligand confers characteristic properties to the metal complexes that they form.

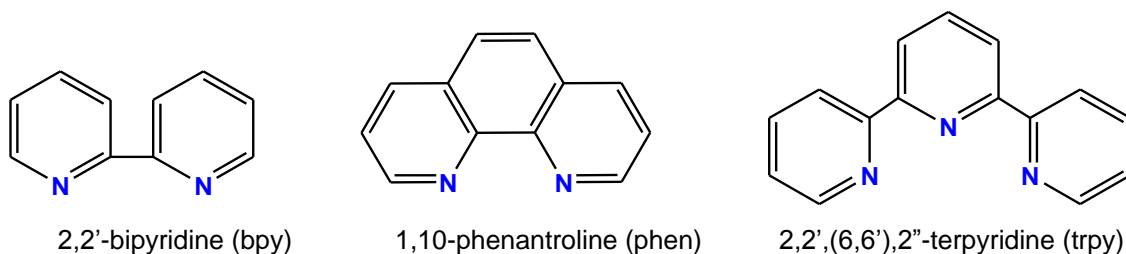
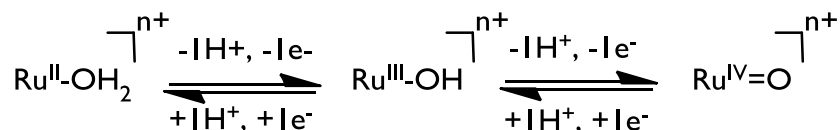


Figure 1. Common polypyridyl ligands used in ruthenium coordination chemistry.

The redox properties of metal polypyridine complexes become especially interesting when aqua ligands are directly bound to the metal center. In this case, a proton-

coupled-electron-transfer (PCET) is achievable, making the high oxidation states more accessible.¹²



Scheme 1. PCET characteristic of ruthenium aqua complexes.

As shown in Scheme 1, PCET is involved in electrochemical reactions where reduction is related to protonation or where oxidation is coupled to deprotonation, so the successive oxidation from Ru(II) to Ru(IV) are accompanied by the sequential loss of protons. Moreover, the initial Ru(II)-OH₂ is oxidized to Ru(IV)=O, passing through a Ru(III)-OH species.

As a consequence of this behavior, the pH medium is directly correlated with the redox potentials of the aqua complexes: if pH increases the Ru(III/II) and Ru(IV/III) couples are shifted to lower potentials. This effect can be demonstrated with the Nernst equation that correlates pH with redox potentials.

$$E_{1/2} = E^{\circ}_{1/2} - 0.059 \cdot (m/n) \cdot \text{pH}$$

Equation 1. Relation between potential and pH in Nernst equation.

m= number of transferred protons, *n*= number of transferred electrons.

In Equation 1 $E_{1/2}$ is the half wave redox potentials at a given pH, $E^{\circ}_{1/2}$ is the half wave redox potential at standard conditions, *m* is the number of transferred protons and *n* is the number of transferred electrons. The dependence of the $E_{1/2}$ value with the pH is commonly represented under the form of *Pourbaix* diagrams.

Finally, the importance of obtaining oxocomplexes with a two-electron process is important because this type of catalyst leads to concerted reactions avoiding a radical mechanism, which can promote undesirable side reactions.¹³

1.3 Ruthenium complexes with sulfoxide ligands

The chemistry of transition metal with sulfoxide ligands increased rapidly after the first article reported in the sixties.¹⁴ These type of complexes have one relevant feature because their most common use is as precursors for the synthesis of a wide range of organometallic and coordination compounds,¹⁵ and their application in a high number of catalytic processes.¹⁶ Nevertheless, the most remarkable application of these complexes is their utility in medical chemistry as antitumor compounds¹⁷ and antimetastatic agents.¹⁸

From the chemical viewpoint, the ambidentate behavior of sulfoxide ligands makes them important due to bond isomerization linkage process, so it makes it interesting from an academic point of view in basic coordination chemistry.¹⁹ For this reason, the understanding of the factors, which affects the bond mode, is important for the study of these complexes.

1.3.1 Ru-dmso bond

As mentioned above, the ambidentate nature of this ligand is a relevant characteristic, given its potential coordination through the O atom or the S atom. We can also find the metal coordination through S atom, although it occurs in particular cases, especially in the second and third metal transition series complexes as the group VIII and some complex of the group VI and VII. This fact depends on different factors such as the metal properties; the other ligands coordinated to the metal and also the steric hindrance.

There are some factors that can provoke the isomerization:

- Changes in metal oxidation state.
- Coordination of π -acceptor ligands (such as CO or CN) in *trans* to S-dmso.
- Thermal or photochemical factors.
- Steric factors that can force the ligand isomerization.

Regarding ruthenium, it belongs to the second series of transition and group VIII, consequently, isomerization processes can occur due to the oxidation of metal atom from Ru(II) to Ru(III).

The Pearson acid-base theory (HSAB) explains the stability of compounds, reaction mechanisms and pathways. Accordingly, the Ru(II) oxidation state (d^6 low spin configuration) has more affinity to S atom given its character of soft Lewis acid (large atomic/ionic radius, high polarizability, low electronegativity...). In contrast, for Ru(III) (d^5 low spin configuration) the coordination via O atom is favored due to the harder Lewis acid nature (small atomic/ionic radius, low polarizability,...).

In accordance with HSAB,²⁰ diffuse orbitals from metallic ions are overlapped with diffuse orbitals from S. Due to the properties of the dmso ligand as a π -acceptor, the metal-S linkage is favored by π -retrodonation from metal to dmso orbitals because the metal stabilizes the S atom ceding electron density to the empty orbitals of dmso. This is the case of Ru(II), which stabilizes the Ru-S bond. In fact, this bond has some double bond character due to the π -retrodonation and as a consequence the Ru-S distances are lower. When a change in the oxidation state is made (from II to III), it is observed a decrease of π -retrodonation that involves an increase of Ru-S distances.

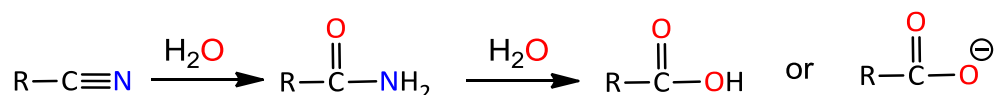
When a bond isomerization of the dmso ligand happens (from Ru-S to Ru-O), it is observed a decrease of the bond order in the S-O linkage. Consequently, there is an increase of the bond distance (Ru-O). In the other hand, the steric effects also can induce the formation of the link through oxygen atom.

1.4 Ruthenium complexes as catalysts

As mentioned above, the ruthenium complexes present several applications in the catalytic field, since they can catalyze a wide range of reactions including reductive and oxidative processes. In this work, the research is centered to study new ruthenium complexes and their application as catalysts for the hydrolysis of nitriles and alkene epoxidation.

1.4.1 Hydrolysis of nitriles

The hydrolysis of nitriles is a very relevant reaction from the pharmacological and industrial point of view because it allows the synthesis of amides (such as the acrylamide and benzamide) or carboxylic acids from the corresponding nitriles, see Scheme 2:



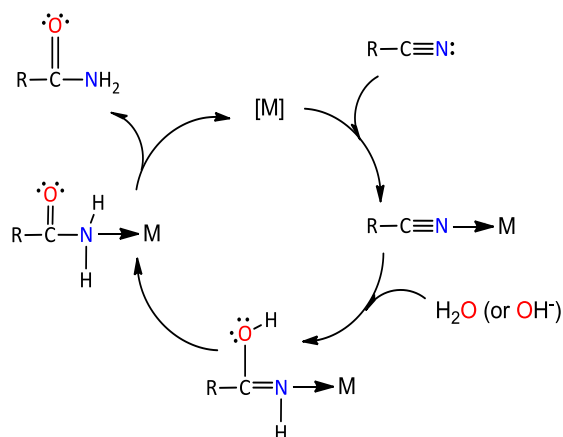
Scheme 2. Nitrile hydrolysis reaction to obtain the amide and, finally the transformation to carboxylic acid.

Originally, strong acids and bases catalyzed the nitrile hydrolysis reaction. This kind of compounds showed some disadvantages:

- The need of control of the temperature and reagents to avoid overheating and polymerizations.
- Formation of salts after the final neutralization of the medium causing their removal difficult.
- Waste generated.
- Low selectivity for the amide due the fast hydrolysis to carboxylic acid (second step of Scheme 2).

For these reasons, the metal catalyst was introduced in the reaction in order to activate the nitrile group, obtaining more selectivity and increasing the reaction rate.

As shown in Scheme 3, the nucleophilic attack of an OH⁻ group takes place thanks to the activation of the nitrile group provided by coordination of this to the metal.

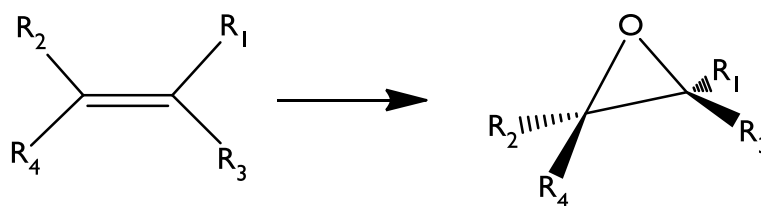


Scheme 3. Mechanism of hydrolysis of nitriles by metal catalyst.

Several reported metal catalysts for nitrile hydrolysis include platinum, rhodium and ruthenium.²¹ Among these, some organometallic and phosphine-containing Ru compounds are widely studied and have demonstrated good efficiency in homogeneous catalysis using pure water as solvent.²²

1.4.2 Alkene epoxidation

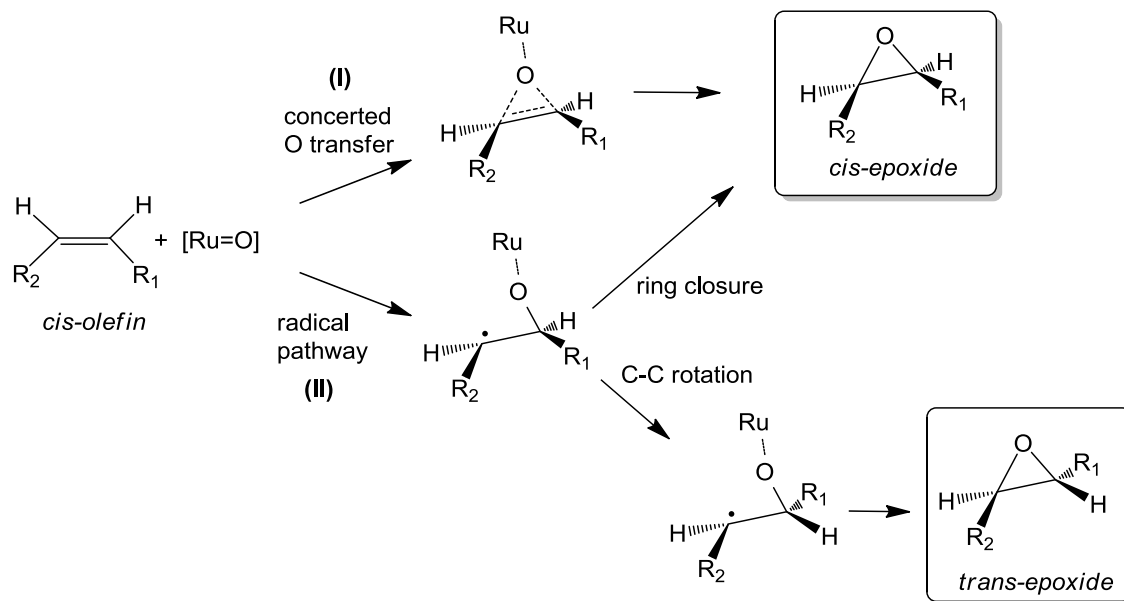
The catalytic epoxidation of alkenes (Scheme 4) has great importance from academics and industry point of view. Olefin epoxidation has an interest due to the fact that epoxides are useful as intermediates in organic reactions and they can be easily transformed to functionalized compounds.²³ Epoxides are used in the synthesis of many industrial products, for example, in fine chemical some anti-inflammatory and anti-allergic agents are synthesized from epoxide.²⁴ Epoxy polymers are widely used in the marine, automotive, aerospace and building industries.



Scheme 4. Alkene epoxidation process.

Ruthenium complexes have been proved to be efficient in the epoxidation of different olefins with relatively high selectivities.²⁵ In general, epoxide yields depend on several factors such as the nature of the substrates, catalysts and reaction conditions.

A key point in ruthenium-mediated epoxidation is the mechanism followed.²⁶ Two general routes have been described, which are depicted in Scheme 5 for a general *cis*-olefin:



Scheme 5. Possible pathways for metal-catalyzed epoxidation.

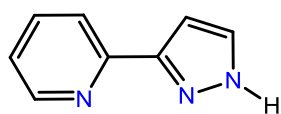
The concerted oxo transfer **(I)** leads to a *stereospecific* epoxidation, keeping the *cis* stereoisomerism of the original alkene in the final epoxide product, whereas the radical pathway **(II)** generates an intermediate species that can either undergo direct ring closure (also leading to the *cis*-epoxide) or, alternatively, it can suffer C-C bond rotation prior to ring closure leading to the *trans*-epoxide, which is thermodynamically more stable. Depending on the relative reaction rates of these processes, the radical mechanism can result in a mixture of *cis*- and *trans*-epoxides.

2. Objectives

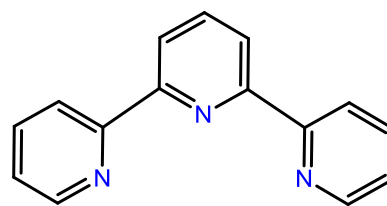
The general objectives of this work were the design of new ruthenium complexes with N-donor ligands and the evaluation of the complexes as catalysts for the nitrile hydrolysis reaction and alkene epoxidation.

The specific objectives are:

- Synthesis and characterization of ruthenium chloro- and aqua-complexes with 2-(3-pyrazolyl)pyridine (pypzH) and 2,2',(6,6'),2"-terpyridine (trpy) ligands, with general formula $[\text{RuX}(\text{trpy})(\text{pypzH})]^{n+}$ ($X = \text{Cl}, \text{H}_2\text{O}$):



pypzH



trpy

- Optimization of the synthetic procedure for the preparation of the chloro-complex through the evaluation of different synthetic pathways.
- Evaluation of the catalytic activity of the ruthenium complexes synthesized for the nitrile hydrolysis and the alkene epoxidation reactions.

3. Experimental section

3.1 Instrumentation and measurements

- *UV-Vis*

UV-Vis spectroscopy was performed on a Cary 50 Scan (Varian) UV-Vis spectrophotometer with 2 mm quartz cells.

- *Cyclic voltammetry (CV) and differential pulse voltammetry (DPV)*

CV and DPV experiments were performed in an IJ-Cambria IH-660 potentiostat using a three electrode cell. Glassy carbon electrode (3 mm diameter) from BAS was used as working electrode, platinum wire as auxiliary and SCE as the reference electrode. The complexes were dissolved in solvents containing the necessary amount of $n\text{-Bu}_4\text{NPF}_6$ (TBAH) as supporting electrolyte to yield a 0.1 M ionic strength solution. All $E_{1/2}$ values reported in this work were estimated from cyclic voltammetric experiments as the average of the oxidative and reductive peak potentials $(E_{p,a}+E_{p,c})/2$, or directly from DPV peaks.

- *IR*

IR spectroscopy was performed on an Agilent Technologies, Cary 630 FTIR equipped with an ATR system, directly on the samples without any previous treatment.

- *NMR spectra*

The NMR spectroscopy was performed on a Bruker DPX 400 MHz. Samples were run in CD_2Cl_2 , and to evaluate the catalytic activity for hydration of nitriles the samples were run in deuterated water.

- *Gas chromatography*

Gas chromatography experiments were performed by capillary GC, using a GC-2010 Gas Chromatograph from Shimadzu, equipped with an Astec CHIRALDEX G-TA Column (30 m x 0.25 mm diameter) incorporating a FID detector. All the product analyses in the catalytic experiments were performed by means of calibration curves using biphenyl as internal standard.

3.2 Synthesis of compounds

The ligand 2-(3-pyrazolyl)pyridine (pypzH)²⁷, $\text{cis-}[\text{RuCl}_2(\text{dmsO})_2(\text{pypzH})]$ [**2**]²⁸ and $[\text{RuCl}_2(\text{dmsO})_4]$ [**1**]²⁹ complexes were prepared according to procedures described in the literature that are detailed below.

Synthesis of the ligand 2-(3-pyrazolyl)pyridine, pypzH

2 g (11.35 mmol) of 3-(dimethylamino)-1-(2-pyridyl)-2-propen-1-one together with 0.72 mL (14.84 mmol) of hydrazine were refluxed in ethanol (20 mL) at 85°C for 1 hour. The mixture was cooled to room temperature. Once cooled, the solvent was evaporated in a vacuum. The brown precipitate corresponds to pypzH. Yield: 1.58 g (79%). **¹H-NMR (400 MHz, CDCl₃):** δ = 6.81 (d, 1H, H5), 7.23 (dd, 1H, H4), 7.66 (d, 1H, H6), 7.74 (ddd, 2H, H2, H3), 8.63 (dd, 1H, H1). For the NMR assignment we have used the numeration scheme displayed in Scheme 6 for the ligand depicted in complex [2].

Synthesis of [RuCl₂(dmsO)₄], [1]

1 g (3.83 mmol) of RuCl₃·2.38H₂O was refluxed in 5 mL of dmsO at 170 °C for 10 minutes. After this time, the solution was cooled to room temperature; 10 mL of acetone were added. The yellow precipitate formed was separated by filtration and successively washed with acetone and ether and dried in vacuum. Yield: 214.8 mg (11%).

Synthesis of *cis*-[RuCl₂(dmsO)₂(pypzH)], [2]

A mixture of [RuCl₂(dmsO)₄] [1] (303 mg, 0.62 mmol), and pypzH (91 mg, 0.62 mmol) was dissolved in 40 mL of ethanol and heated at 90°C under nitrogen atmosphere for 2 hours. After the reaction time, the solution was cooled to room temperature and the volume was reduced in a rotary evaporator. The yellow precipitate formed (corresponds to compound [2]) was separated by filtration and successively washed with ether and dried in vacuum. Yield: 130 mg (43%). **¹H-NMR (400 MHz, CD₂Cl₂):** δ = 2.00 (s, 3H, H11), 2.92 (s, 3H, H10), 3.52 (s, 3H, H9), 3.54 (s, 3H, H8), 6.99 (d, 1H, H5, *J*_{5,6}=2.8Hz), 7.54 (ddd, 1H, H2, *J*_{2,1}=6.8Hz; *J*_{2,3}=7.4Hz; *J*_{2,4}=1.5Hz), 7.79 (d, 1H, H6, *J*_{6,5}=2.8Hz), 7.95 (ddd, 1H, H4, *J*_{4,3}=7.4Hz; *J*_{4,2}=1.5Hz; *J*_{4,1}=0.9Hz), 8.02 (t, 1H, H3, *J*_{3,2}=*J*_{3,4}=7.4Hz; *J*_{3,1}=1.5Hz), 9.44 (ddd, 1H, H1, *J*_{1,2}=6.8Hz; *J*_{1,3}=1.5Hz; *J*_{1,4}=0.9Hz), 13.11 (s, 1H, H7). For the NMR assignments we have used the numeration scheme in Scheme 6. *E*_{1/2} (III/II) (CH₂Cl₂ + 0.1 M TBAH): 1.15 V vs. SCE.

Synthesis of [RuCl₃(trpy)], [3]

The synthesis of [RuCl₃(trpy)] [3]³⁰ was prepared according to the procedure described in the literature.

To 50 mL of absolute ethanol, 104 mg (0.39 mmol) of RuCl₃·3H₂O and 92 mg (0.39 mmol) of 2,2':6,2''-terpyridine were added. The mixture was heated at reflux for 3 hours. After this time the reaction was cooled to room temperature, and the fine brown powder which had appeared was filtered. The product was washed with ether and dried in vacuum. Yield: 152 mg (87%).

Synthesis of [RuCl₂(dmsO)(trpy)], [4]

The synthesis of [RuCl₂(dmsO)(trpy)] [4]³¹ was performed through a modification of the method previously described in the literature.

0.250 g (0.516 mmol) of $[\text{RuCl}_2(\text{dmsO})_4]$ [**1**], and 0.123 g (0.516 mmol) of 2,2':6,2''-terpyridine were dissolved in 40 mL of absolute ethanol, and the resulting solution was refluxed for 2 h. A dark solid, corresponding to the mixture of *trans*- and *cis*- $[\text{RuCl}_2(\text{dmsO})(\text{trpy})]$ in a 1: 0.5 ratio, was formed in solution and was filtered on a frit and washed with ether. A brown solid was obtained by reducing the volume of the mother liquor to 15 mL, and this solid corresponds to a mixture of *trans*- and *cis*- $[\text{RuCl}_2(\text{dmsO})(\text{trpy})]$ in a 0.4:1 ratio. Yield: 200.8 mg (80 %). **¹H-NMR (400 MHz, CD₂Cl₂):** δ = 2.75 (s, 3H, H6, H7), 3.75 (s, 6H, H6, H7), 7.45 (ddd, 2H, H9, H17), 7.62 (ddd, 1H, H9, H17), 7.85 (m, 3H, H10, H13, H16), 8.02 (m, 2H, H8, H10, H16, H18), 8.06 (dd, 1H, H13), 8.13 (dd, 2H, H8, H18), 8.18 (dd, 1H, H12, H14), 8.20 (dd, 2H, H12, H14), 9.27 (dd, 1H, H11, H15), 9.32 (dd, 2H, H11, H15). For the NMR assignments we have used the numeration scheme in Scheme 6. ***E*_{1/2} (CH₂Cl₂ + 0.1 M TBAH):** 0.89 V Ru(IV/III) and 0.46 V Ru(III/II) vs. SCE.

3.2.1 Synthesis of $[\text{RuCl}(\text{trpy})(\text{pypzH})](\text{PF}_6)$, [**5**]

Complex [**5**] was prepared following three different pathways.

Pathway A

A mixture of sample [**2**] (74.3 mg, 0.157 mmol) and 2,2':6,2''-terpyridine (37 mg, 0.157 mmol) were refluxed in methanol (25 mL) at 60°C under N₂ atmosphere for 48 hours. Once the reaction time was over, the solution was cooled to room temperature and the volume was reduced in a rotary evaporator. Then, a saturated aqueous solution of NH₄PF₆ was added and a brown precipitate formed was separated by filtration and washed with ether and dried in vacuum. The solid obtained in this manner was purified by basic alumina column chromatography eluting with methylene chloride (increasing polarity with methanol). Yield: 48%. **¹H-NMR (400 MHz, CD₂Cl₂):** δ = 6.75 (d, 1H, H5), 7.14 (ddd, 2H, H9, H17), 7.33 (d, 1H, H6), 7.63 (ddd, 3H, H2, H8, H18), 7.75 (ddd, 2H, H10, H16), 7.95 (ddd, 1H, H3), 8.04 (dd, 2H, H4, H13), 8.16 (dd, 2H, H11, H15), 8.28 (dd, 2H, H12, H14), 10.13 (dd, 1H, H1). For the NMR assignments we have used the numeration scheme in Figure 2. **IR (ν_{max} , cm⁻¹):** 3800-3000 (w), 3200-2800 (m). ***E*_{1/2} (III/II) (CH₂Cl₂ + 0.1 M TBAH):** 0.84 V vs. SCE. **UV-vis (CH₂Cl₂):** λ_{max} , nm (ϵ , M⁻¹ cm⁻¹) 275 (10304), 322 (7684), 408 (2040), 500 (1945).

Pathway B

0.1 g (0.23 mmol) of sample [**3**] and 6 equivalent of LiCl (0.6 g) were mixed with 15 mL of ethanol:water (9:1) adding 0.1 mL of Et₃N at room temperature for 30 minutes under N₂ atmosphere. In parallel, 32.9 mg (0.23 mmol) of pypzH were dissolved in 5 mL of ethanol:water (9:1) under N₂ atmosphere. After 30 minutes, these reactions were joined at 90°C under N₂ atmosphere for 2 hours. After the reaction time has passed, the reaction was cooled to room temperature and the volume was reduced in a rotary evaporator. Afterwards, a saturated aqueous solution of NH₄PF₆ was added and a brown precipitate formed was separated by filtration and washed with ether and dried in vacuum. The solid obtained in this manner was a mixture of $[\text{RuCl}(\text{trpy})(\text{pypzH})]\cdot\text{PF}_6$ and $[\text{Ru}(\text{trpy})(\text{pypzH})\text{OH}_2]\cdot(\text{PF}_6)_2$. The mixture is purified by basic alumina column

chromatography eluting with methylene chloride, increasing polarity with methanol. Yield: 80%.

Pathway C

150 mg (0.34 mmol) of complex **[4]** and 49 mg (0.34 mmol) of ligand pypzH were solved in 20 mL of absolute ethanol under N₂ atmosphere for 22 hours. After the reaction time, the mixture was cooled to room temperature and the volume was reduced. Then, a saturated aqueous solution NH₄PF₆ was added and a brown precipitate formed was separated by filtration and washed with ether and dried in vacuum. The solid obtained in this manner was a mixture of [RuCl(trpy)(pypzH)]·PF₆, [Ru(trpy)(pypzH)OH₂](PF₆)₂ and [Ru(dmsO)(trpy)(pypzH)]·PF₆. The mixture is purified by basic alumina column chromatography eluting with methylene chloride and increasing polarity with methanol. Yield: 57%.

3.2.2 Synthesis of *trans*-[Ru(H₂O)(trpy)(pypzH)](PF₆)₂, **[6]**

The aqua-complex **[6]** can be obtained through solubilization of 10 mg of *trans*-chloro-complex **[5]** in 5 ml of water for 20 hours at room temperature. After this time the solid was isolated by adding 1 ml of a saturated aqueous solution of NH₄PF₆. **¹H-NMR (400 MHz, D₂O):** δ = 7.04 (d, 1H, H5), 7.34 (t, 2H, H9, H17), 7.42 (d, 1H, H6), 7.85 (d, 2H, H8, H11), 7.91 (t, 1H, H2), 7.93 (t, 2H, H10, H16), 8.20 (t, 1H, H13), 8.28 (t, 1H, H3), 8.32 (d, 1H, H4), 8.45 (d, 2H, H12, H14), 9.44 (d, 1H, H1). For the NMR assignments we have used the numeration scheme in Figure 2. **E_{1/2}** (phosphate buffer pH = 7): 0.69 V (Ru(IV/III)) and 0.40 V (Ru(III/II)) vs SCE. **UV-vis** (CH₂Cl₂): λ_{max}, nm (ε, M⁻¹ cm⁻¹) 386 (5386), 462 (6118).

3.2.3 Catalytic experiments

3.2.3.1 Hydrolysis of nitriles

These experiments have been carried out using several nitrile substrates under neutral conditions in water as a solvent at 80°C. They have been performed using a Ru-catalyst:substrate ratio of 1:100. The remaining substrate has been quantified through GC analysis employing biphenyl as an internal standard and the selectivities have been analyzed by NMR spectroscopy on the reaction crude as detailed below.

0.01 mmol of complex **[5]** was dissolved in 3 mL of water and 1 mmol of the substrate (benzonitrile or acrylonitrile) was added. The mixture was heated at 80°C for 20 hours in a catalysis reactor under stirring. After the reaction time, three different extractions with 2 mL of chloroform (first of this containing biphenyl as an internal standard) were performed in order to collect the non-reacted nitrile. In one hand, the organic phase was analyzed by GC, determining the nitrile conversion. On the other, the aqueous phase remained at room temperature until the water was evaporated. The solid obtained from this phase was analyzed by NMR spectroscopy in order to determine the selectivity of the final product.

3.2.3.2 Alkene epoxidation

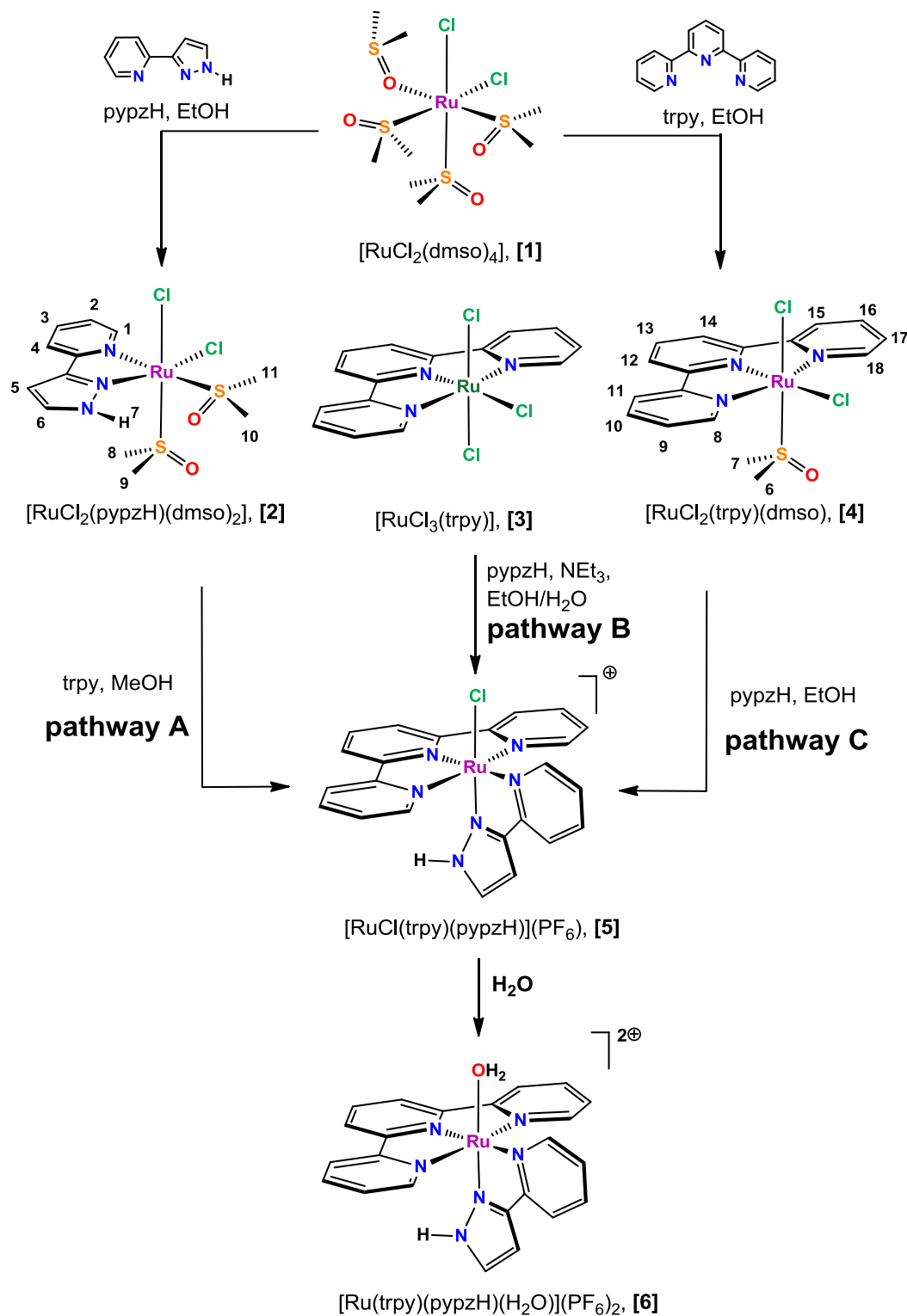
The catalytic activity of the ruthenium was checked in the epoxidation of *cis*- β -methylstyrene and *cis*-cyclooctene in dichloromethane and using iodobenzene diacetate as oxidant. These catalytic reaction has been performed using a [Ru-Catalyst:Substrate] ratio of 1.25 μ mol:125 μ mol. The remaining substrate has been quantified through GC analysis employing biphenyl as an internal standard.

1.25 μ mol of catalyst **[5]**, 125 μ mol of the substrate and 250 μ mol of PhI(OAc)₂ were stirred at room temperature in 2.5 mL of CH₂Cl₂ for 24 hours. After the addition of an internal standard, the sample was filtered through a basic alumina plug and quantified by GC analysis.

4. Results and discussion

4.1 Synthesis and structures

The synthetic pathways leading to complexes **[2]**-**[6]** is depicted in Scheme 6:



Scheme 6. Schematic pathways to synthesize complex **[5]** and the aqua-complex **[6]**.

Complex **[1]** is used to synthesize complex **[2]** and **[4]** with ligands pypzH and trpy in ethanol. Complex **[3]** was synthesized from RuCl₃ with trpy ligand in ethanol/water (not shown in Scheme 6). Complex **[2]**, **[3]** and **[4]** were characterized by CV, UV-Vis, IR and ¹H-RMN and the results obtained are in accordance with those published in the literature.

As mentioned above, the complex **[5]** can be synthesized using three different pathways. The pathways are distinguished from each other in the order of the introduction sequence of the ligands (pypzH and trpy).

Once the complex **[5]** is formed, is easy to obtain the aqua-complex **[6]** in water during 20 hours at room temperature. It is interesting to remark that a similar complex³² containing the corresponding N-methylated pypz-Me ligand does not display this ligand exchange process in water and the addition of a silver salt is necessary to remove the chloro ligand. This difference can be due to the higher electron-donor capacity of the pypzH ligand that can undergo a deprotonation process in water as described below, then exerting a labilizing effect on the coordinated Cl ligand.

Besides, the structures of the two formed isomers of complex **[5]** are shown in Figure 2.

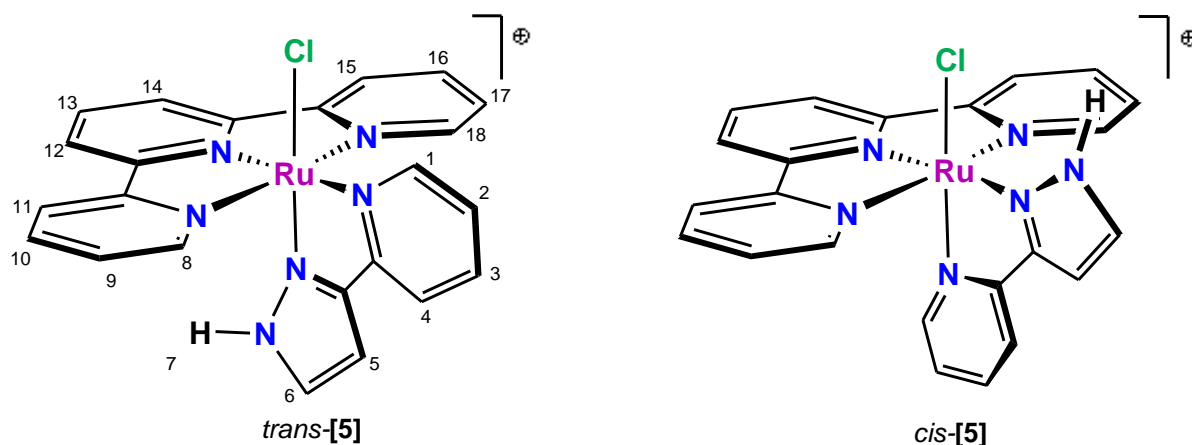


Figure 2. Possible isomers for complex **[5]**.

In the different chloro-complex **[5]** pathways, an equimolar mixture of *cis:trans* isomers was obtained, but when a purification by column chromatography was performed the isomer *trans* was isolated easily, in contrast with isomer *cis* that was mixed with a small portion of the isomer *trans*.

4.2 Spectroscopic properties

4.2.1 IR spectroscopy

IR spectra have been registered for complex **[5]**. The more relevant factor of IR spectra is the presence of the significant bands in 3800-3300 cm⁻¹ range indicating the

presence of a N-H bond and, in 3200-2800 cm^{-1} range corresponding to the aromatic C-H bond.

4.2.2 NMR spectroscopy

The $^1\text{H-NMR}$ spectra studies for the ligand (pypzH) shows seven signals. The spectra showed that the two carbon protons of pyrazole have the same pick appearance and the nitrogen proton has the higher chemical shift due to the proximity to the N atom of the pyrazole which is an electronegative atom (sometimes this proton pick does not appear because the proton exchanges with deuterium atom of the solvent). In the other hand, the proton 2 also has a high chemical shift, and the last three protons of pyridine are shown in the aromatic range. The $^1\text{H-NMR}$ spectra for the ligand (pypzH) is displayed in the Figure 3.

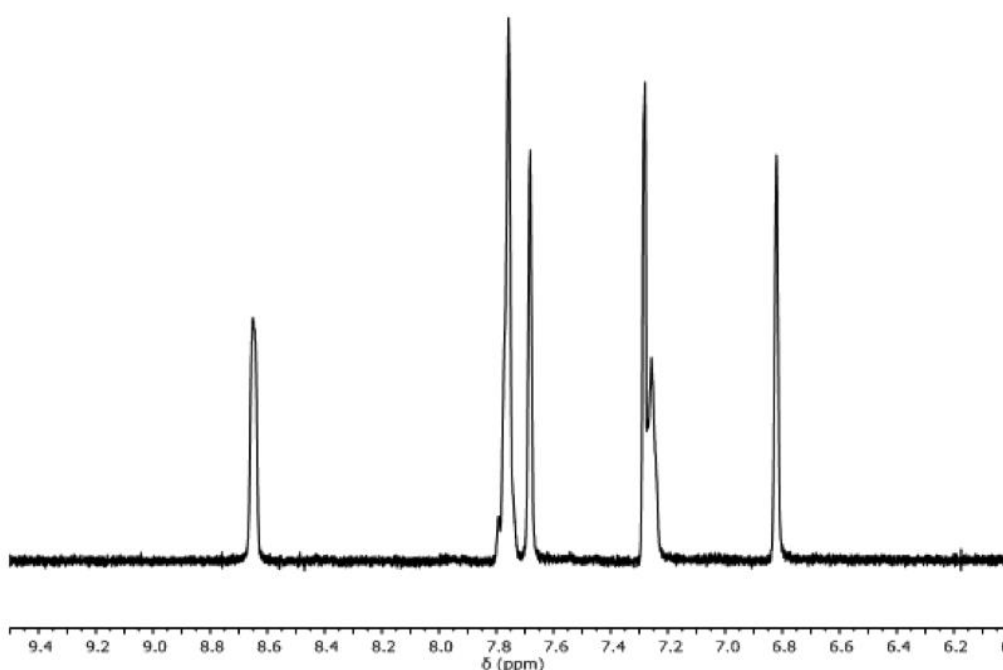


Figure 3. $^1\text{H-NMR}$ for ligand pypzH registered in CDCl_3 .

For complex **[2]** (Figure 4) we can find the aromatic protons of the ligand pypzH in the aromatic region and the protons of methyl group of dmsoligand in the aliphatic region. If we compare this spectra with the one in literature we can confirm that the complex is *cis*, so the chloro ligands are placed in *cis*.

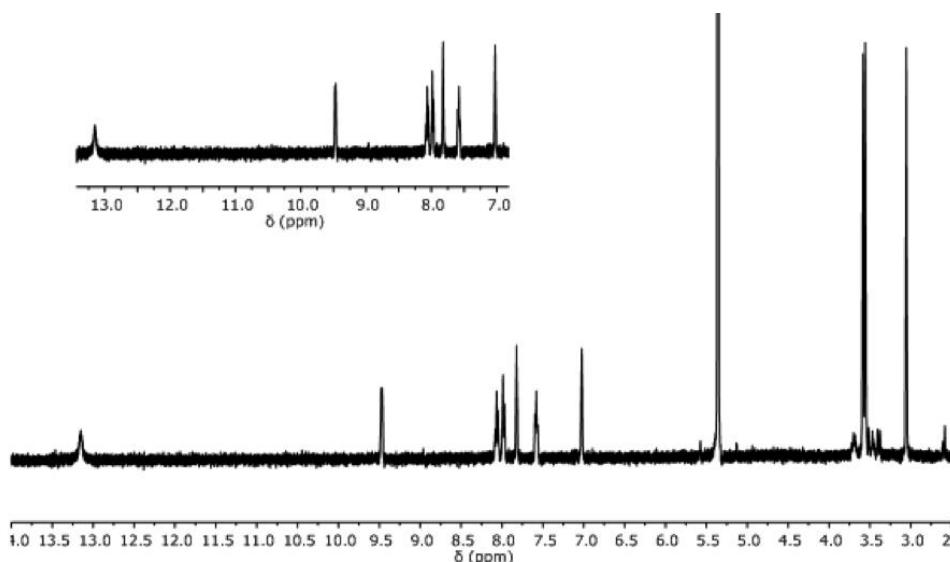


Figure 4. $^1\text{H-NMR}$ for complex [2] registered in CD_2Cl_2 .

For complex [4], we can assign all the protons thanks to the literature as it is obtained in a *trans*:*cis* ratio of 1:0.5. As it can be seen below, for the *cis* isomer five aromatic signals are identifiable, however, for the *trans* isomer we find six aromatic signals. Some aromatic signals are overlapped and have been difficult to assign. The signals corresponding to the *trans* isomer are marked with red squares, and the signals corresponding to the *cis* isomer are marked in blue squares. Besides the aromatic signals we can find the aliphatic signals corresponding to the methyl groups of dmsoligand.

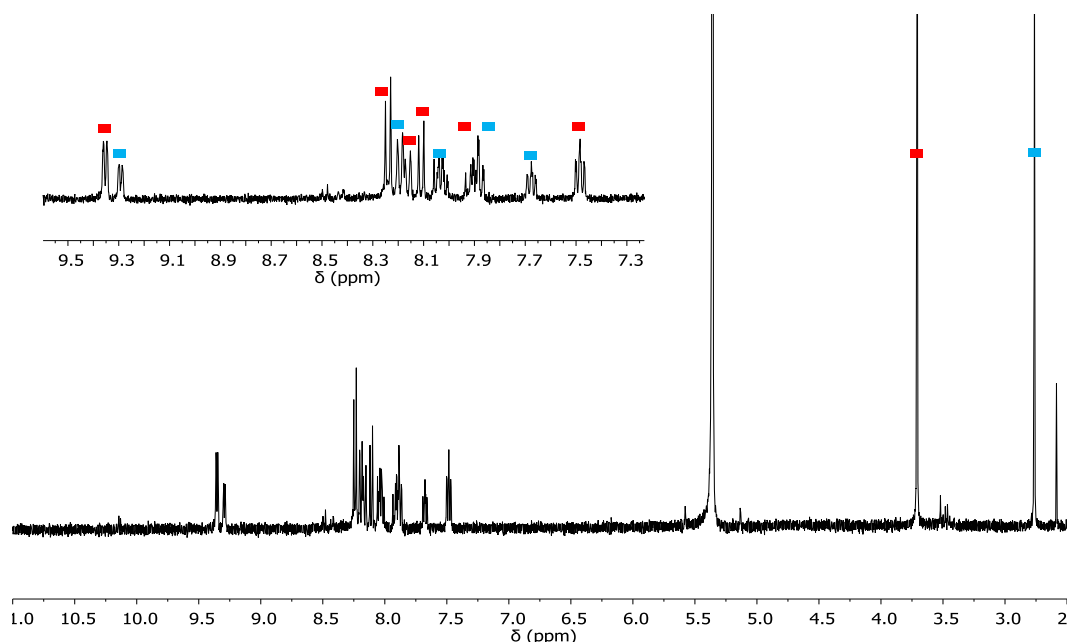


Figure 5. $^1\text{H-NMR}$ for complex [4] registered in CD_2Cl_2 .

In the $^1\text{H-NMR}$ spectra for complex *trans*-[5] (Figure 6) we can assign all the protons thanks to NOESY and COSY spectra except the nitrogen proton of the pyrazole possibly because he had exchanged for deuterium from the solvent. As it discussed

above, the proton 2 of the pyridine has a high chemical shift, in this case the higher chemical shift. In the aromatic region we can find all the protons of the trpy and ligand pypzH. For the assignation of the protons we have relied on the multiplicities and the ligand pypzH spectra. According to the chemical shift, it has been confirmed that the isomer formed is the *trans* (see Figure 2), so the pyridyl ring of the ligand pypzH is in *cis* with the chlorine atom.

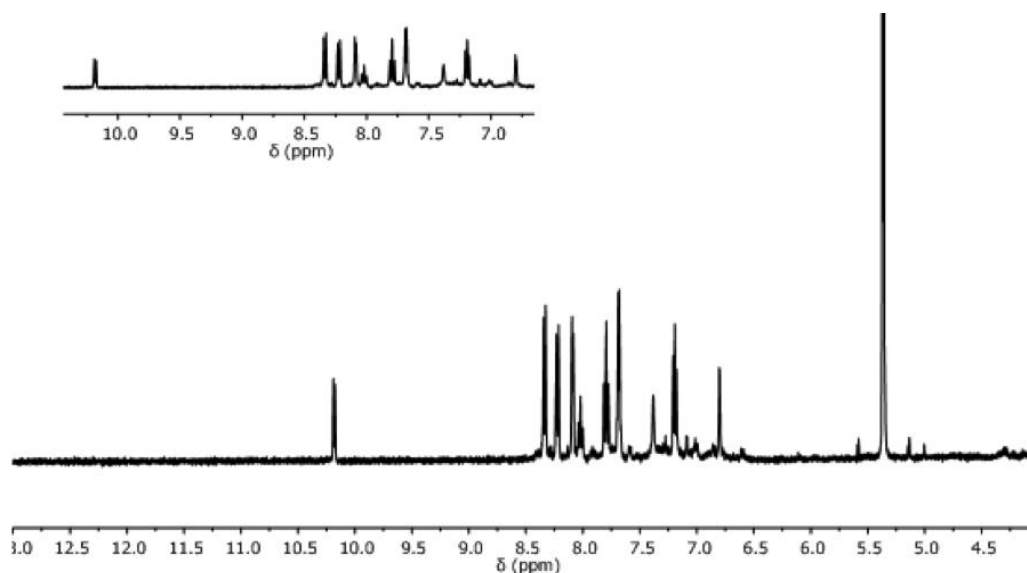


Figure 6. $^1\text{H-NMR}$ for complex [5] registered in CD_2Cl_2 .

For complex [6], we can assign all the protons due to structural similarity to the complex [5]. The higher chemical shift corresponds to the proton next to the nitrogen atom of the pyridine of the pypzH ligand. The pyrazole proton doesn't appear and we can find all the protons in the aromatic region that correspond with the ligands protons. According to the chemical shift, the isomer formed is *trans*, so the pyridine of the ligand pypzH was in *cis* with the aqua ligand.

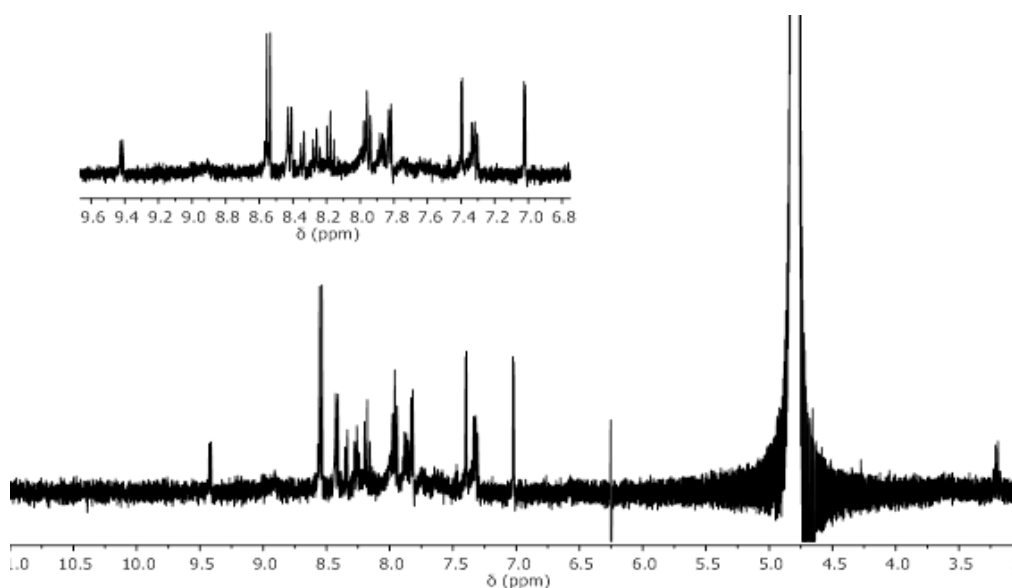


Figure 7. $^1\text{H-NMR}$ for complex [6] registered in D_2O .

4.2.3 UV-Vis spectroscopy

The UV-Vis spectrum of complex **[5]** has been performed in CH_2Cl_2 and is displayed in Figure 8. The complex exhibits relatively intense bands between 340 and 540 nm assigned to metal-to-ligand $d\pi-\pi^*$ charge transfers (MLTC). Furthermore, the complex presents intraligand $\pi-\pi^*$ absorptions in lower wavelengths.

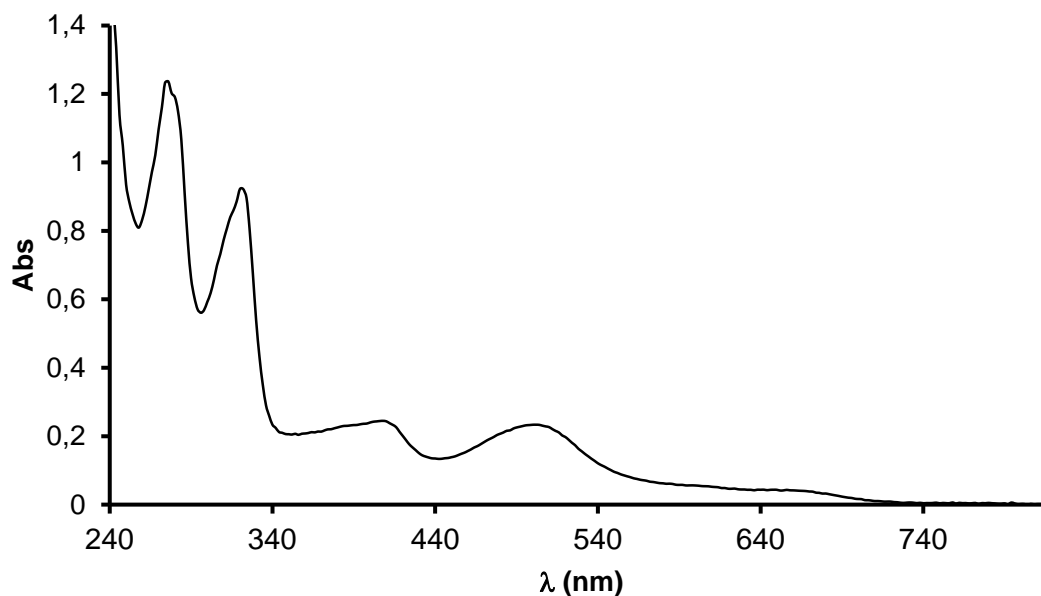
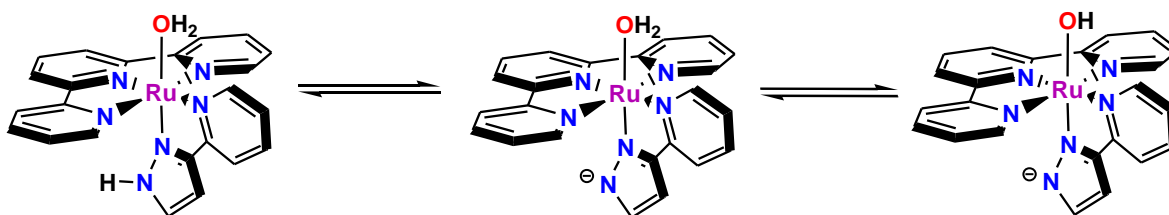


Figure 8. UV-Visible spectra of a $8 \cdot 10^{-5}$ M solution of complex **[5]** in CH_2Cl_2 .

4.2.4 Acid-base spectrophotometric titration of complex **[6]**

As described previously, complex **[6]** can be easily obtained through solubilization of chloro-complex **[5]** in water. Complex **[6]** can undergo two independent acid-base transformations: one involving the N-H bond of pypzH ligand and a second one where the aqua ligand is deprotonated.



Scheme 7. Aqua-complex with and without proton and hydroxo-complex.

These transformations can be followed through UV-vis spectroscopy because deprotonation produces a shift in the λ values in accordance with the electron donor and acceptor capacity of the ligands (related with their position in the spectrochemical series), with the more electron-donating ligands producing a displacement to longer λ absorptions.

For the spectrophotometric assay, on the basis of similar ligands described previously,³³ we can expect the pKa for the pypzH ligand to be around 6-7. Therefore we must ensure that we have the protonated ligand in the starting point. For this reason we start from a $1.5 \cdot 10^{-4}$ M solution of *trans*-[5] in nitric acid at pH 1 (Figure 9). The solution is stirred to complete the hydrolysis of the chlorocomplex to the aquacomplex [6]. During this time the solution changes the color from brown to orange. For the chloro-complex the MLTC bands are shifted to longer wavelengths (red shift) with regard to the corresponding aqua-complex because of the relative destabilization of the $d\pi-\pi^*$ provoked by the anionic chloro ligand..

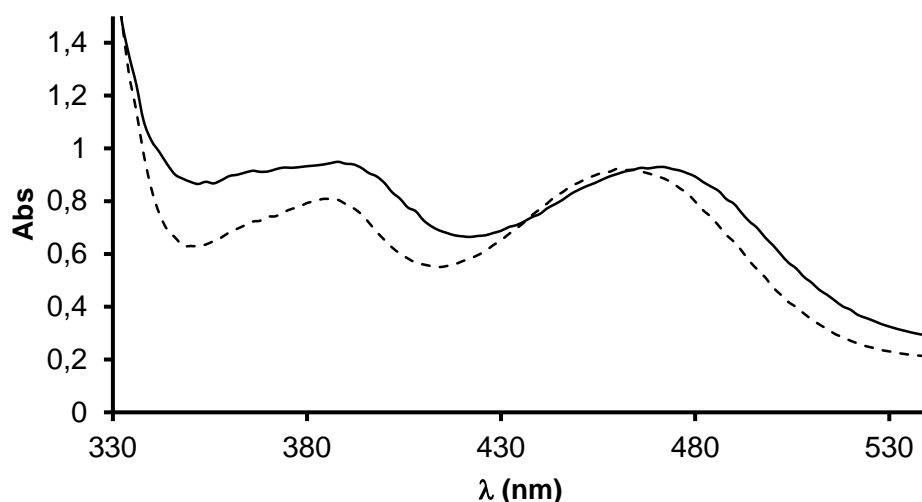


Figure 9. UV-Vis spectra corresponding to the formation of complex [6] (dashed line) from complex [5] (solid line).

To follow the deprotonation process on complex [6], a 4M solution of NaOH is added progressively to complete 4 equivalents of base. The assay shows the variation of the UV-Vis bands changing the pH of the solution. In Figure 10 we can see the shift of the wavelength when we change the pH from 5 until 9.13. Two isosbestic points at 480 nm and 412 nm are clearly seen, indicating the net conversion from the aquacomplex with protonated and deprotonated pypzH ligand.

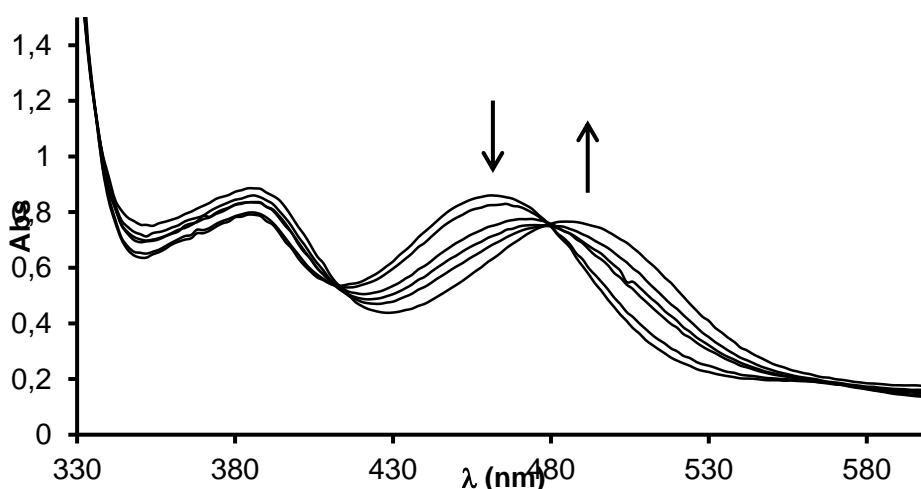


Figure 10. UV-Vis spectra at pH 5-9.13 upon addition of NaOH. Isosbestic points are found at 412 nm and 480 nm.

If we continue adding NaOH at pH from 9.25 to 11 a new set of spectra are observed, corresponding to the formation of a hydroxo-complex, which means that the deprotonation of the aquo ligand is performed (Figure 11).

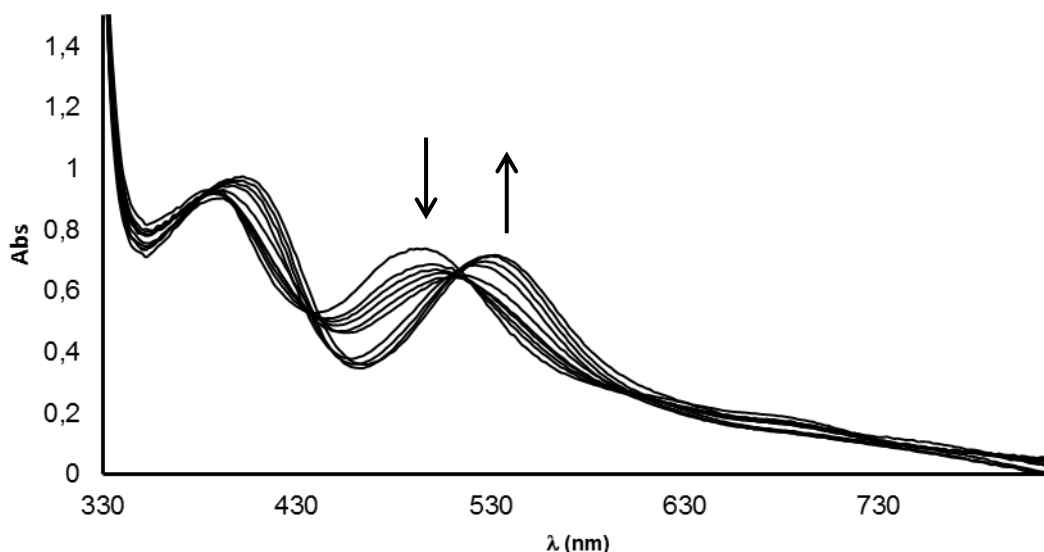


Figure 11. UV-Vis spectra at pH 9.25-11.

In Figure 11 the isosbestic points are not well defined, probably due to the co-existence of the three species displayed in Scheme 7.

In both figures 10 and 11 the shift to higher λ values found after deprotonation indicate a larger electron-donor capacity of the ligands bound to Ru that destabilizes the $d\pi$ orbitals of Ru, thus leading to lower energy MLCT transitions.

4.3 Electrochemical properties

Cyclic voltammetry (CV) experiments have been performed to study the redox properties of complex **[5]** and complex **[6]**.

The CV registered for **[5]** in CH_2Cl_2 (Figure 12) exhibits a reversible Ru(III)/Ru(II) redox wave at $E_{1/2} = 0.84$ V with SCE as the reference electrode. This potential is consistent with the formation of the chloro-complex **[5]** by comparison of its $E_{1/2}$ value with similar complexes previously described.^{32,33a}

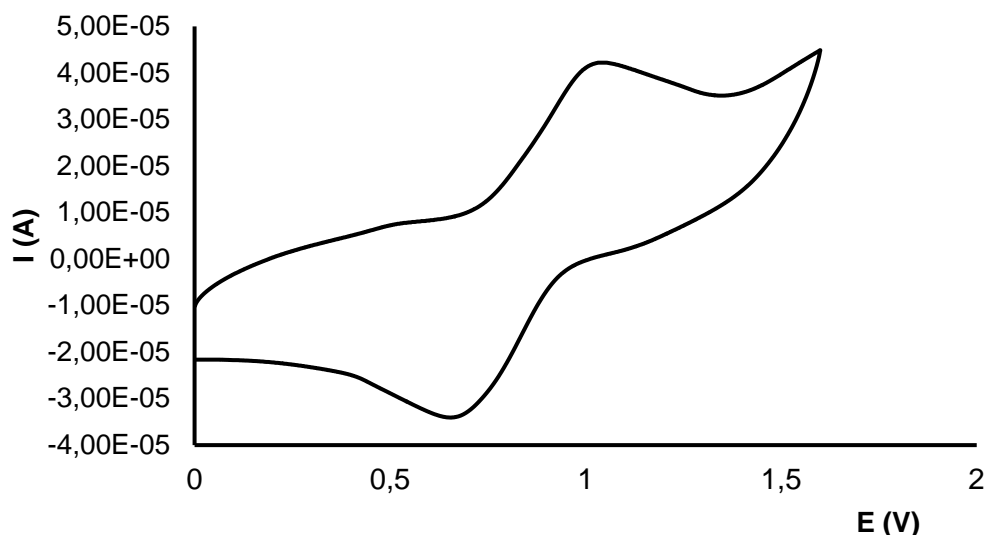


Figure 12. CV for complex [5] registered in CH_2Cl_2 .

The CV registered in phosphate buffer at pH 7 for complex [6] (Figure 13) exhibits a reversible Ru(III)/Ru(II) redox wave at $E_{1/2} = 0.4 \text{ V}$ and a Ru(IV)/Ru(III) wave at $E_{1/2} = 0.69 \text{ V}$ with SCE as the reference electrode.

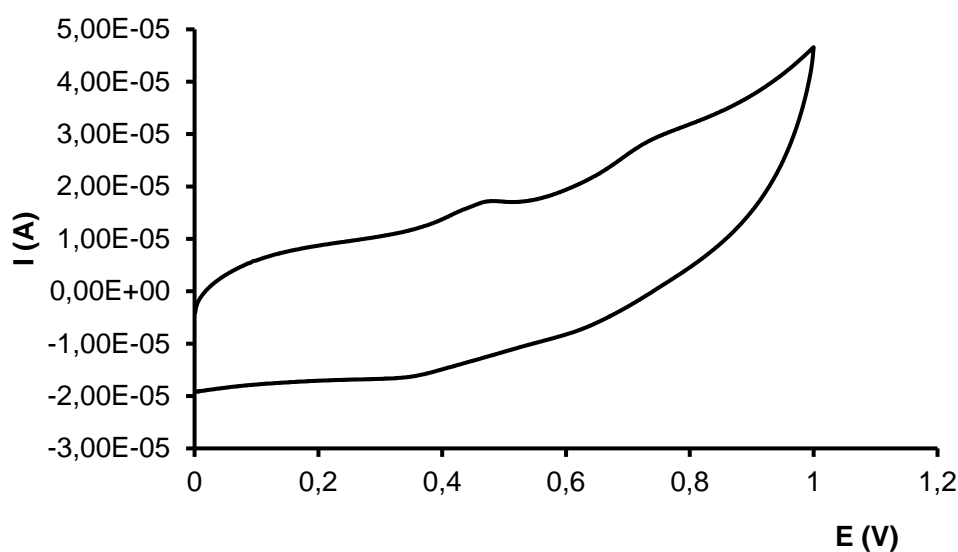


Figure 13. CV for complex [6] registered in phosphate buffer at pH 7.

The dependence of the $E_{1/2}$ values with respect to pH can be represented in the form of *Pourbaix* diagrams. Figure 14 displays the diagram corresponding to the aquacomplex *trans*-[6] where the vertical dotted lines represent the pK_a values for the different acid-base equilibria involved, and the solid lines are visual guides for the evolution of the $E_{1/2}$, which are represented as solid squares. The proton composition of the different chemical species is also indicated, with for instance " $\text{Ru}^{\text{II}}(\text{pzH})(\text{OH}_2)$ " representing the complex *trans*- $[\text{Ru}(\text{H}_2\text{O})(\text{trpy})(\text{pypzH})](\text{PF}_6)_2$ under its reduced, fully protonated form,

“Ru^{II}(pz)(OH₂)” is the corresponding Ru(II) form with deprotonated pyridyl-pyrazolate ligand, etc.

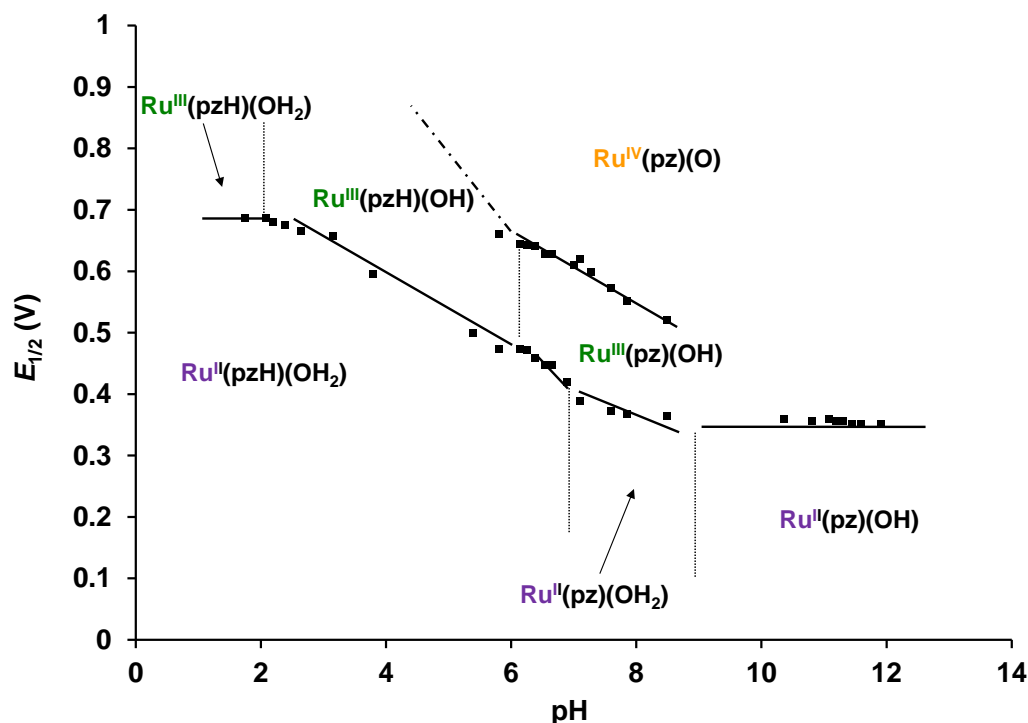


Figure 14. Pourbaix diagram for complex *trans*-[6]. The stability zones and the proton composition for the different redox species are indicated.

The complex presents two main redox processes corresponding to the Ru(IV/III) and Ru(III/II) redox pairs, as described above from the cyclic voltammetry (Figure 13). The slope of the solid lines depends on the number of protons and electrons exchanged, as inferred from Nernst equation (Eq. 1). Thus, the equilibrium between “Ru^{II}(pzH)(OH₂)” and “Ru^{III}(pzH)(OH)” involves the exchange of one proton and one electron and will therefore display a slope of 59 mV per pH unit. In a similar way, the equilibrium between “Ru^{II}(pzH)(OH₂)” and “Ru^{III}(pz)(OH)” exchanges one electron and two protons with a slope of approximately 118 mV per pH unit.

As can be observed, in the Ru(II) oxidation state the deprotonation of the pyridylpyrazole ligand takes place at pH around 7 and the aqua ligand is deprotonated at pH above 9. For the Ru(III) species the analogous processes take place at lower pH (below 6 for the pyrazole deprotonation and at around 2 for the aqua ligand deprotonation), due to the higher Lewis acidity of the Ru(III) metal center compared to Ru(II). The reduction of the pK_a value upon increasing the oxidation state is particularly remarkable in the case of the aqua ligand since it is directly bound to the Ru metal center.

4.4 Catalytic activity

4.4.1 Hydrolysis of nitriles

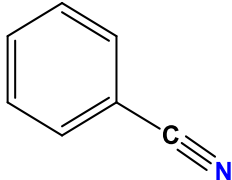
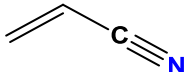
As mentioned above, the hydration of nitriles in order to generate the corresponding amide is an important reaction from industrial and pharmacological points of view. Traditionally this reaction was carried out in acidic and basic conditions but presented some drawbacks. The metal complexes are good candidates as catalysts due to activation of the CN bond. For this reason, complex [5] has been tested as catalyst in the catalytic hydration process.

This process has been assessed using benzonitrile and acrylonitrile as substrates. The reaction has been performed at 80°C during 20 hours using a 1:100 Ru-catalyst:substrate ratio and water as solvent.

The remaining, non-reacted nitrile has been quantified, after chloroform extraction, through GC chromatography using biphenyl as the internal standard and, finally the hydrolysis product has been analyzed by NMR spectroscopy and compared to pure samples of the corresponding amides. The results of conversion and selectivity values for complex [5] are summarized in Table 1.

The values obtained in hydration of nitriles show an excellent selectivity for both substrates because the carboxylic acid is not found in any case when analyzing the hydrolysis products by NMR spectroscopy. The conversion value for benzonitrile as a substrate is very good, in contrast to the conversion obtained for the substrate acrylonitrile using [5] as a catalyst that shows a moderate value.

Table 1. Ru-catalyzed hydration of nitriles to amides in water using catalyst [5].

Substrate	Conversion (%)	Selectivity (%)
	82	>99
	38	>99

As mentioned above, the catalytic hydration of nitriles involves a substitution process, where a ligand of the complex is replaced by the nitrile and finally there is a nucleophilic attack of water (or hydroxo anions) on the nitrile carbon. The ability of the metal to activate the nitrile is influenced by the electronic characteristics and steric factors of the ligands. Comparing the two substrates is interesting to observe that when benzonitrile is used as the substrate, higher conversion values than acrylonitrile are obtained. This may be explained with the resonance delocalization of the aromatic ring that presents the benzonitrile, which activates the nucleophilic attack on the nitrile

carbon. It seems that the electronic factors govern the reactivity because the bulkier substrate (but more activated) works better.

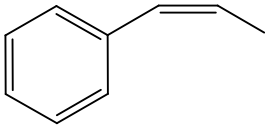

It is expectable that the catalytic active species is in this case the aquacomplex [6] since chloro ligand substitution takes place in complex [5] after solubilization, as described above. Also, the coordination site left by the amide product once formed (see Scheme 3) will be more likely occupied by a water solvent molecule to start a subsequent catalytic cycle.

4.4.2 Alkene epoxidation

This process has been assessed using 1-cicloocten and *cis*- β -methylstyrene as substrates. The reaction has been performed at 25°C during 24 hours using $\text{PhI}(\text{OAc})_2$ as an oxidant, a Ru-catalyst:substrate ratio of 1:100 and CH_2Cl_2 as solvent. The remaining substrate has been quantified through GC analysis and employing biphenyl as an internal standard.

In Table 2 the catalytic results are shown.

Table 2. Ru-catalyzed alkene epoxidation using catalyst [5].

Substrate	Conversion (%)	Selectivity (%)
	63	>99
	>99	>99

Comparing the two substrates is interesting to observe that when 1-cicloocten is used as the substrate, higher conversion values than *cis*- β -methylstyrene are obtained. This can suggest that the catalytic active species is electrophilic since the more electron-rich aliphatic olefin is oxidized faster. It is important to remark that the selectivity for the epoxide is excellent in both cases, and in case of *cis*- β -methylstyrene the process was stereospecific yielding 100% *cis* epoxide, so we cannot discard any mechanism of the reaction (see Scheme 5 in the introduction). The mechanism could be an oxygen atom transferred directly through a concerted oxene insertion or a one-electron breakage of the C=C bond resulting in the formation of an acyclic intermediate, where the ring closure was faster than the *cis* \rightarrow *trans* rotation.

4.5 Ethical and sustainability issues

From the ethical and sustainability point of view, this project presents some advantages and disadvantages. First of all, according to the twelve principles of green chemistry, some are presented as:

- Principle 8 “*Reduce Derivatives*”: Unnecessary derivatization should be minimized or avoided if possible, because such steps require additional

reagents and can generate waste. We did not use blocking or protection/deprotection groups, therefore syntheses were shorter.

- Principle 9 “*Catalysis*”: Catalytic reagents (as selective as possible) are superior to stoichiometric reagents. For the hydrolysis of nitriles and the alkene epoxidation the amount of complex **[5]** was speck.

In the other hand, the disadvantages that present and could be modified are:

- Principle 5 “*Safer solvents and auxiliaries*”: The use of auxiliary substances should be made unnecessary wherever possible and innocuous when used (as VOC compounds, such as methanol, ethanol, CH₂Cl₂ and others, that favoring the formation of ozone layer lower atmosphere. These solvents were used to purify complex **[5]**).
- Principle 7 “*Use of renewable feedstocks*”: A raw material or feedstock should be renewable rather than depleting whenever technically and economically practicable. For example, the use of ethanol that previously was obtained by the carbohydrates fermentation.

5. Conclusions

The synthesis and characterization of the precursor Ru complexes **[2]**-**[4]** with π -acceptor pypzH and trpy ligands has been achieved and the complexes have been used to synthesize complex $[\text{RuCl}(\text{pypzH})(\text{trpy})](\text{PH}_6)$, **[5]**, through three different pathways. The route B, starting from complex **[3]**, leads to better yield than pathways **A** and **C**.

Complex **[5]** is obtained as a mixture of *cis* and *trans* isomers.

The aqua-complex **[6]** is formed *in situ* through solubilization of complex **[5]** in water, as demonstrated by UV-vis spectroscopy. This behavior might be favored by the electron-donor capacity of the deprotonated pypz ligand.

Complex **[6]** displays two pH-dependent redox processes corresponding to the Ru(IV/III) and Ru(III/II) redox pairs. The Pourbaix diagram indicates that two deprotonation processes can take place, corresponding to the deprotonation of the pypzH and aqua ligands. These two processes occur at lower pH values in the corresponding Ru(III) oxidation state and it is particularly manifested in the case of the aqua ligand, directly bound to the metal.

Complex **[5]** has been evaluated as catalyst in the hydration of nitriles in neutral conditions using water as a solvent and benzonitrile and acrylonitrile as substrates. The conversion displayed for benzonitrile is better than for acrylonitrile, but both substrates achieve excellent selectivities for the amide product. The catalytic process seems to be governed by electronic factors because the bulkier substrate, but more activated works well than acrylonitrile. It is likely that complex **[5]** is transformed into **[6]** under the catalytic conditions.

In the other hand, complex **[5]** has been also evaluated as catalyst in the alkene epoxidation using CH_2Cl_2 as a solvent for 1-cicloocten and *cis*- β -methylstyrene as substrates. It displays a good conversion for both substrates, in special for 1-cicloocten, which could be in accordance with the occurrence of an electrophilic catalytic species. The selectivities are excellent for both substrates, and the complex is stereospecific in the case of the *cis* olefin, which does not allow us to discard any of the potential mechanisms of activity.

6. References

- ¹ Qu, P.; Thompson, D. W.; Meyer, G. J. *Langmuir* **2000**, *16*, 4662.
- ² Seok, W. K.; Meyer, T. J. *Inorg. Chem.* **2005**, *44*, 3931.
- ³ Ley, S. V.; Norman, J.; Griffith, W. P.; Marsden, S. P. *Synthesis* **1994**, *7*, 639.
- ⁴ Coe, B. J. *Coord. Chem. Rev.* **2013**, *257*, 1438.
- ⁵ Fillaut, J.; Andriès, J.; Marwaha, R. D.; Lanoë, P.; Lohio, O.; Toupet, L.; Gareth Williams, J. J. *Organomet. Chem.* **2008**, *693*, 228.
- ⁶ Mikuriya, M.; Yoshioka, D.; Handa, M. *Coord. Chem. Rev.* **2006**, *250*, 2194.
- ⁷ Yoshida, J.; Watanabe, G.; Kakizawa, K.; Kawabata, Y.; Yuge, H. *Inorg. Chem.* **2013**, *52*, 11042.
- ⁸ Zhang, S.; Ding, Y.; Wei, H. *Molecules* **2014**, *19*, 11933.
- ⁹ Belser, P.; De Cola, L.; Hartl, F.; Adamo, V.; Bozic, B.; Chriqui, Y.; Iyer, V. M.; Jukes, R. T. F.; Kühni, J.; Querol, M.; Roma, S.; Salluce, N. *Adv. Funct. Mater.* **2006**, *16*, 195.
- ¹⁰ Xie, P.-H. Hou, Y.-J.; Wei, T.-X.; Zang, B.-W.; Cao, Y.; Huang, C.-H. *Inorg. Chim. Acta* **2000**, *308*, 73.
- ¹¹ Delaney, S.; Pascaly, M.; Bhattacharya, P. K.; Han, K.; Barton, J. K. *Inorg. Chem.* **2002**, *41*, 1966.
- ¹² Costentin, C.; Robert, M.; Saveant, J.-M. *Chem. Rev.* **2010**, *110*, PR1-PR40.
- ¹³ Masllorens, E.; Rodríguez, M.; Romero, I.; Roglans, A.; Parella, T.; Benet-Buchholz, J.; Poyatos, M.; Llobet, A. *J. Am. Chem. Soc.* **2006**, *128*, 5306.
- ¹⁴ Cotton, F. A.; Francis, R. J. *Inorg. Nucl. Chem.* **1961**, *17*, 62.
- ¹⁵ Mola, J.; Romero, I.; Rodríguez, M.; Bozoglian, F.; Poater, A.; Sola, M.; Parella, T.; Benet-Buchholz, J. *Inorg. Chem.* **2007**, *46*, 10707.
- ¹⁶ Wang, L.; Duan, L.; Stewart, B.; Pu, M.; Liu, J.; Privalov, T.; Sun, L. *J. Am. Chem. Soc.* **2012**, *134*, 18868.
- ¹⁷ Alessio, E.; Mestroni, G.; Nardin, G.; Attia, W. M.; Calligaris, M.; Sava, G.; Zorzet, S. *Inorg. Chem.* **1988**, *27*, 4099.
- ¹⁸ a) Sava, G.; Pacor, S.; Mestroni, G.; Alessio, E. *Clin. Exp. Metastasis* **1992**, *10*, 273.
b) Bratsos, L.; Jedner, S.; Gianferrara, T.; Alessio, E. *Chimia* **2007**, *61*, 692.
- ¹⁹ Alessio, E.; Macchi, M.; Heath, S. L.; Marzilli, L. G. *Inorg. Chem.* **1997**, *36*, 5614.
- ²⁰ Komiyama, S.; Susuki, S.; Watanabe, K.; *Bull. Chem. Soc. Jpn.* **1971**, *44*, 1440.
- ²¹ Ahmed, T. J.; Knapp, S. M. M.; Tyler, D. R. *Coord. Chem. Rev.* **2011**, *255*, 949.
- ²² a) Tomás-Mendivil, E.; Cadierno, V.; menéndez, M. I.; López, R. *Chem. Eur. J.* **2015**, *21*, 16874. b) Fung, W. K.; Huang, X.; Man, M. L.; Ng, S. M.; Hung, M. Y.; Lin, Z.; Lau, C. P. *J. Am. Chem. Soc.* **2003**, *125*, 11539. c) Cadierno, V.; Diez, J.; Francos, J.; Gimeno, J. *Chem. Eur. J.* **2010**, *16*, 9808. d) García-Álvarez, R.; Zablocka, M.; Crochet, P.; Duhayon, C.; Majoral, J.-P.; Cadierno, V. *Green Chem.* **2013**, *15*, 2447.
- ²³ Banu, A.; Stan, R.; Matondo, H.; Perez, E.; Rico-Lattes, I.; Lattes, A. *C. R. Chim.* **2005**, *8*, 853.
- ²⁴ Upjohn, *J. Am. Chem. Soc.* **1956**, 6213.
- ²⁵ a) Dakkach, M.; Atlamsani, A.; Parella, T.; Fontrodona, X.; Romero, I.; Rodríguez, M. *Inorg. Chem.* **2013**, *52*, 5077. b) Aguiló, J.; Francàs, L.; Bofill, R.; Gil-Sepulcre, M.; García-Antón, J.; Poater, A.; Llobet, A.; Escriche, L.; Meyer, F.; Sala, X. *Inorg. Chem.* **2015**, *54*, 6782. c) Dakkach, M.; Atlamsani, A.; Parella, T.; Fontrodona, X.; Romero, I.;

Rodríguez, M. *Adv. Synth. Catal.* **2011**, 353, 231. d) Barf, G. A.; Sheldon, R. A. *J. Mol. Catal. A: Chem.* **1995**, 98, 143.

²⁶ a) Dhuri, S. N.; Cho, K.-B.; Lee, Y.-M.; Shin, S. Y.; Kim, J. H.; Mandal, D.; Shaik, S.; Nam, W. *J. Am. Chem. Soc.* **2015**, 137, 8623. b) Masllorens, E.; Rodríguez, M.; Romero, I.; Roglans, A.; Parella, T.; Benet-Buchholz, J., Poyatos, M.; Llobet, A. *J. Am. Chem. Soc.*, **2006**, 128, 5306.

²⁷ Brunner, H.; Scheck, T. *Chem. Ber.* **1992**, 124,701.

²⁸ Ferrer, I.; Rich, J.; Fontrodona, X.; Rodríguez, M.; Romero, I. *Dalton Trans.* **2013**, 42, 13461.

²⁹ Evans, I. P.; Spencer, A.; Wilkinson, J.J; *J. Chem. Soc., Dalton Trans.* **1973**, 2, 204.

³⁰ Sullivan, B. P.; Calvert, J. M.; Meyer, T. J. *Inorg. Chem.* **1980**, 19, 1404.

³¹ Ziessel, R.; Grosshenny, V.; Hissler, M.; Stroh, C. *Inorg. Chem.* **2004**, 43, 4262.

³² Dakkach, M.; López, M. I.; Romero, I.; Rodríguez, M.; Atlamsani, A.; Parella, T.; Fontrodona, X.; Llobet, A. *Inorg. Chem.* **2010**, 49, 7072.

³³ a) Sens, C.; Rodríguez, M.; Romero, I.; Llobet, A.; Parella, T.; Benet-Buchholz, J. *Inorg. Chem.* **2003**, 42, 8385. b) Sens Llorca, C (2005). *New mono- and dinuclear ruthenium complexes containing the 3,5-bis(2-pyridyl)pyrazole ligand. Synthesis, characterization and applications*. PhD Dissertation, Universitat de Girona. Departament de Química. ISBN 84-689-2580-2.